Clinical Sonopathology for the Regional Anesthesiologist

Part 1: Vascular and Neural

Brian D. Sites, MD, Alan J.R. Macfarlane, MBChB, MRCP, FRCA,† Vincent R. Sites, MD,‡ Ali M. Naraghi, MD, FRCR,§ Vincent W.S. Chan, MD, FRCPC,|| John G. Antonakakis, MD,¶ Mandeep Singh, MBBS, MD,|| and Richard Brull, MD, FRCPC||*

Abstract: The use of ultrasound to facilitate regional anesthesia is an evolving area of clinical, education, and research interests. As our community's experience grows, it has become evident that anesthesiologists performing "routine" ultrasound-guided blocks may very well be confronted with atypical or even pathologic anatomy. As an educational resource for anesthesiologists, the following articles present examples of common sonopathology that may be encountered during ultrasound-guided regional anesthesia. This present article describes sonopathology related to blood vessels and nerves.

(*Reg Anesth Pain Med* 2010;35: 272–280)

When an anesthesiologist scans a patient with ultrasound during the performance of a peripheral nerve block, there is a distinct possibility that a "textbook image" will not be present. Nerves and key reference structures may be hard to distinguish from surrounding soft tissues. There are many potential reasons for this including the laws of physics (eg, artifacts), incorrect machine settings, nuances of patient anatomy, incorrect scanning techniques, and pathologic conditions. Many of the educational objectives and training efforts occurring on national and international levels focus on image optimization through "knobology" issues and scanning techniques. However, little information exists in the literature describing abnormal findings that may be encountered during the conduct of ultrasound-guided regional anesthesia (UGRA). Such pathology or atypical anatomy as seen with ultrasound is referred hereon as sonopathology.

This 2-part article presents a collection of sonopathology that was acquired during a 7-year period at 5 separate institutions. Part 1 addresses common pathologic conditions affecting the tissues most central to UGRA; that is, blood vessels and nerves. Part 2 describes important pathology related to surrounding structures including the viscera and subcutaneous tissues. The information can be considered an extension of the content offered in the 2 articles previously published on ultrasound-related artifacts.[1,2] The primary objective was to expand the educational resources available to anesthesiologists participating in UGRA. The cases and discussions provided in the article will hopefully support the notion that anatomic variation and pathology do occur and will be encountered within the context of our scope of practice. The authors do not support the use of ultrasound as a mass screening examination by anesthesiologists. We recognize that not every case presented in the article will be seen or be relevant to all practitioners. We do believe, however, that the identification of abnormal tissue or challenging anatomy presents a distinct opportunity for anesthesiologists to alter the anesthetic plan, contribute to the medical care of the patient, and potentially avoid certain complications.

VASCULAR

Blood vessels are commonly used as landmarks for UGRA. Short-axis imaging of blood vessels reveals round anechoic structures that are either pulsatile (arteries) or compressible (veins). Blood vessels are generally easy to identify and the target nerve(s) usually lie in close proximity. Vascular lesions, however, can create difficulties for the anesthesiologist either by impeding the intended needle trajectory to the nerve or by displacing the nerve.[3] Both intravascular and perivascular pathology may be encountered during preprocedural scanning. Color Doppler imaging complements 2-dimensional findings and can help to determine patency, vessel narrowing, and perturbations in blood flow. The identification of vascular pathology may have important implications for anesthetic management.

Atherosclerosis

Atherosclerosis affects up to 10% of the Western population older than 65 years, although the true incidence is difficult to quantify because it is often asymptomatic. Up to 10% of adults older than 80 years have greater than 50% carotid artery stenosis.[4] The carotid bifurcation, the most common site for carotid plaques, occurs at the level of the thyroid cartilage. Plaques are often calcified and, therefore, may create distinct acoustic dropout shadows (Fig. 1). Some plaques may be hypoechoic and only noticeable if there is an area absent of color flow within the vessel circumference. Plaques that appear echolucent are lipid-rich, whereas echogenic plaques have a higher content of fibrous tissue and calcification. Diagnostic scanning for plaques is generally performed using vascular long-axis imaging to search for a stenotic lesion along the length of the vessel. Short-axis scanning, as is performed for interscalene blocks, still allows for detection of an eccentric plaque. In the lower limb, the superficial femoral artery (Figs. 2 and 3) is the most common location for atherosclerosis, with popliteal atherosclerotic disease being less prevalent.[5]

From the *Department of Anesthesiology, Dartmouth-Hitchcock Medical Center, Lebanon, NH; †Department of Anaesthesia, Glasgow Royal Infirmary, Scotland, UK; ‡Department of Radiology, Lahey Clinic, Burlington, MA; §Joint Department of Medical Imaging of University Health Network and Mount Sinai Hospital, Toronto Western Hospital, Toronto, Ontario, Canada; ||Department of Anesthesia and Pain Management, Toronto Western Hospital, University Health Network, Toronto, Ontario, Canada; and ¶Department of Anesthesiology, University of Virginia, Charlottesville, VA.

Accepted for publication August 8, 2009.

Address correspondence to: Richard Brull, MD, FRCPC, Department of Anesthesia and Pain Management, Toronto Western Hospital, 399 Bathurst St, Toronto, Ontario, Canada M5T 2S8 (e-mail: richard.brull@uhn.on.ca).

The authors did not receive funding for this study and have no conflict of interest to declare.

ISSN: 1098-7339
DOI: 10.1097/AAP.0b013e3181ddd1f8

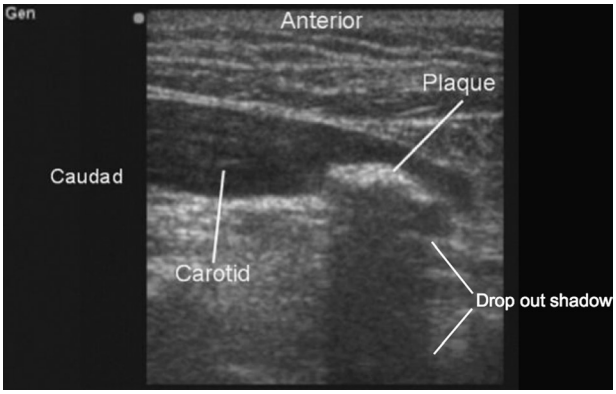

FIGURE 1. Long-axis image of the common carotid artery during the performance of an interscalene block. The anesthesiologists incidentally noticed the hyperechoic lesion just proximal to the carotid bulb. Notice the distinct acoustic dropout shadow created by the calcified plaque.

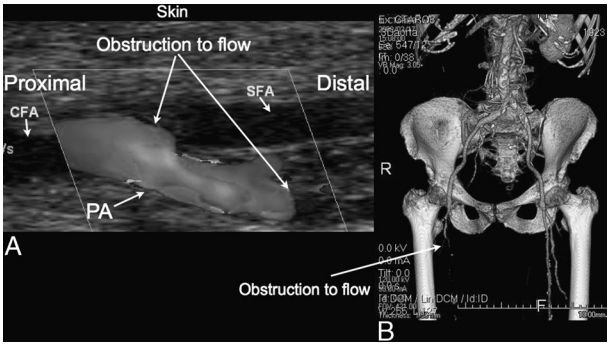

FIGURE 3. A, Long-axis image demonstrating obstruction to flow at the bifurcation of the right common femoral artery. Notice the abrupt ceasing of blood flow as displayed by color Doppler at the SFA/CFA junction and within the profundus. CFA indicates common femoral artery. B, Reconstructed 3-dimensional computed topography (CT) angiogram confirming the findings of the ultrasound examination.

Carotid thrombosis can complicate a preexisting atherosclerotic plaque, as seen in Figure 4. Of note, the thrombosis is not fully appreciated until the operator transitions from the short-axis view (Fig. 4A) to the long-axis view (Fig. 4B). Arterial thrombosis tends to appear homogenous and hyperechoic. However, thrombosis is usually less echogenic than calcium-rich plaques. This difference is clearly evident by comparing Figures 1 and 4B.

Figure 5 is an example of a Doppler phenomenon called aliasing. Aliasing can be identified when using color Doppler in areas of stenosis that generate turbulent and high-velocity flows. Aliasing appears as a mosaic of colors representing flow that exceeds the scale set on the ultrasound machine. Aliasing can be a distinct clue that there is vascular pathology present.

Formal quantification of vascular stenosis by ultrasound is highly accurate and involves standard 2-dimensional imaging, analysis of Doppler waveform, and blood velocity measurements.[6] Ultrasound can also provide information on plaque morphology, giving insight into the risk of embolism (ie, mobile plaque).

The incidental detection of both femoral and carotid arterial plaques has already been reported during scanning for femoral and interscalene nerve blocks, respectively.[7] In each instance, the anesthetic and/or surgical management was altered. Figure 1 is an example of a carotid plaque incidentally found during the performance of an interscalene block. The detection of this lesion in a hypertensive patient scheduled for shoulder surgery resulted in cancellation with a view to improving blood pressure control and arranging a formal investigation. The case later proceeded with invasive arterial monitoring, strict perioperative blood pressure control, altered patient positioning, and the use of intraoperative electroencephalography monitoring. In another example, on detecting a femoral artery plaque in a patient presenting for total knee arthroplasty, it was jointly decided by the surgery and anesthesia teams not to use a tourniquet during the procedure.[7]

The most useful (and simplest) clue for the anesthesiologist indicating the presence of vascular pathology is the identification of a hyperechoic area within the lumen of a blood vessel that is associated with a dropout shadow. If a dropout shadow is noted, consider changing the machine settings from a musculoskeletal application to a vascular-specific setting and lowering the gain to help reduce artifactual speckles within the vessel lumen. These adjustments may help to exclude a false-positive

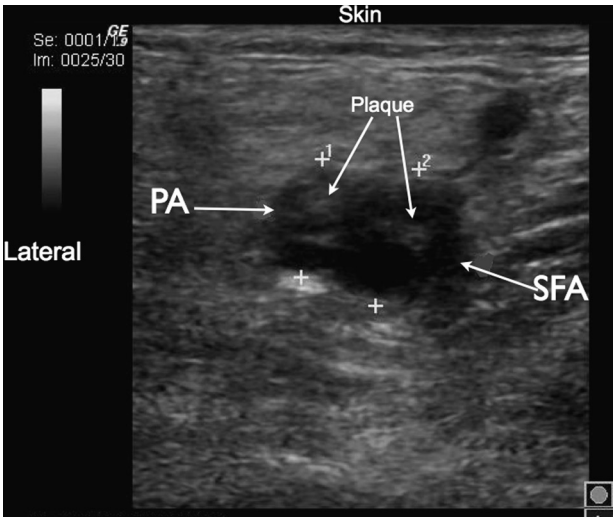

FIGURE 2. Short-axis image demonstrating a thrombus at the bifurcation of the common femoral artery. PA indicates profundus artery; SFA, superficial femoral artery. The plus signs in the image are from the sonographer using machine caliper software to make precise vessel diameter measurements. Thrombi tend not to be as dramatic when imaged in short-axis in comparison to the long-axis (Fig. 3).

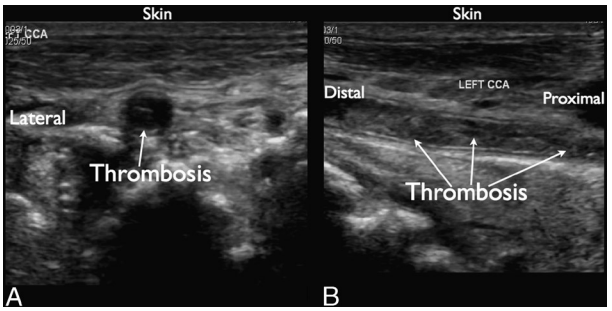

FIGURE 4. A, Short-axis image demonstrating a thrombus in the common carotid artery (CCA). B, Long-axis image of the same CCA demonstrating the extent of the thrombus.

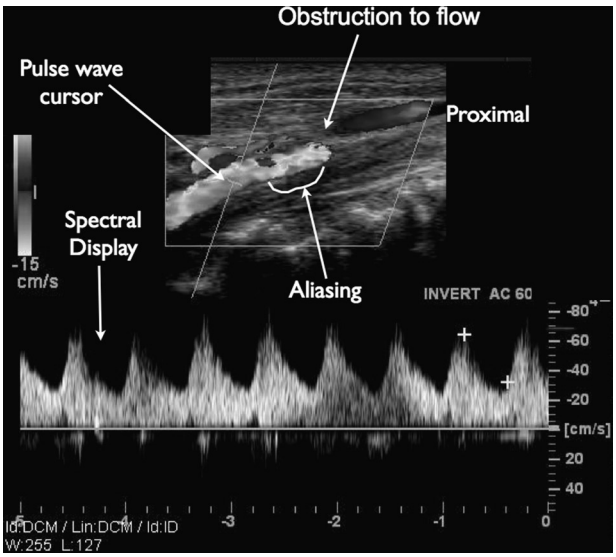

FIGURE 5. Long-axis view demonstrating the obstruction to blood flow in the internal carotid artery causing aliasing on color Doppler. Aliasing can be a sign that indicates turbulent and high-velocity flow associated with a stenosis. This carotid artery is also being analyzed with pulse wave Doppler. Pulse wave Doppler simply measures blood flow velocity at a particular point as indicated by the cursor on the screen that the operator could move. The velocities instead of being mapped with color (color Doppler) are presented as a spectral display (bottom part of image). In such a spectral display, the x-axis is time and the y-axis is velocity in centimeters per second (cm/sec).

diagnosis of a vessel lesion. Also, long-axis imaging of suspected vascular pathology will provide more information than the standard short-axis view.

Deep Venous Thrombosis

The venous drainage system of the lower limb consists of the superficial (great and small saphenous veins) and the deep

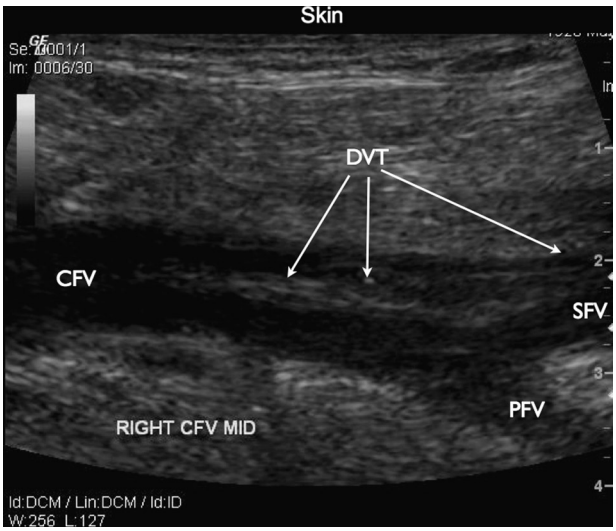

FIGURE 6. Long-axis image demonstrating a large thrombus extending from the superficial femoral vein to the common femoral vein. CFV indicates common femoral vein; PFV, profundus femoral vein; SFV, superficial femoral vein.

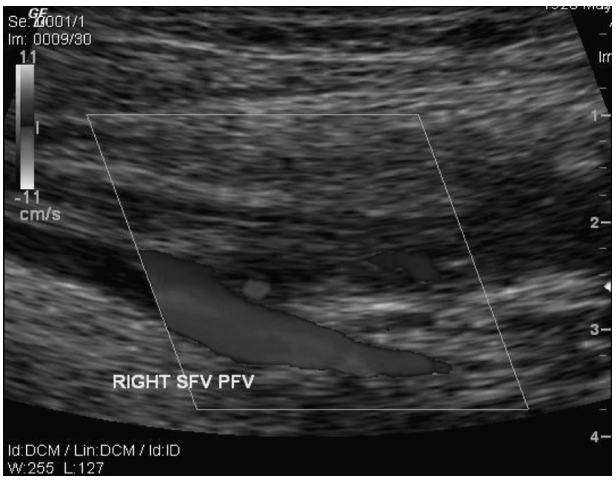

FIGURE 7. Doppler analysis of the same patient as in Figure 6. This image demonstrates obstruction to blood flow as suggested by color Doppler. The large thrombus is evident, extending from the superficial to the common femoral vein.

(tibial, peroneal, popliteal, and femoral veins) systems, connected by perforating and transfascial veins. The incidence of deep venous thrombosis (DVT) varies between particular patient populations.[8] The femoral and popliteal deep veins are commonly imaged by anesthesiologists and can contain acute thrombi.[9] Classically, a venous thrombus presents (in short-axis) as a noncompressible and often dilated circle of variable echogenicity. There will likely be an absent or obstructed blood flow.[10] Sonographic findings will change depending on the age of the thrombosis. In general, a fresh thrombus is hypoechoic and homogenous with an associated dilated, incompressible vein. A chronic thrombus may shrink and become more hyperechoic and heterogeneous.

The incidental finding of a DVT during ultrasound scanning for regional anesthesia has already been documented.[7,11] In 1 case, an inferior vena cava filter was inserted before surgery.[11] Figure 6 demonstrates a dramatic thrombosis of the common femoral vein as seen in long-axis imaging. This DVT

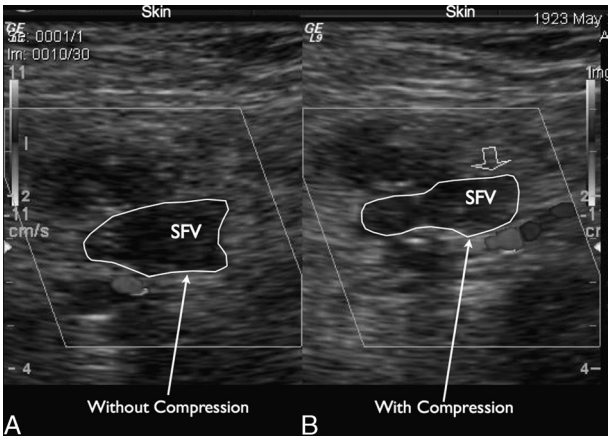

FIGURE 8. Venous thrombus in the SFV. Notice the lack of vessel compressibility and absent blood flow with Doppler analysis. Lack of dynamic compressibility with the transducer during ultrasound analysis is considered a hallmark of a DVT.

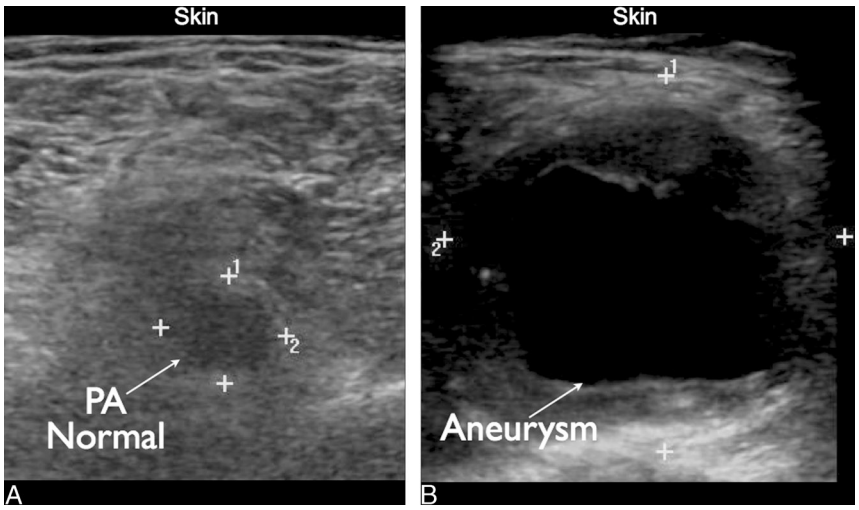

FIGURE 9. Popliteal aneurysm. A, Normal popliteal artery approximately 5 cm proximal to the popliteal crease. B, Short-axis image of an aneurysm in the same patient at the level of the popliteal crease. This lesion could easily be detected in the context of performing a popliteal sciatic block.[4] PA indicates popliteal artery. The plus signs are part of the machine software used by the sonographer to measure vessel diameter.

has extended proximally from the superficial femoral vein to the common femoral vein. Doppler analysis can help confirm the lack of blood flow secondary to an obstruction (Fig. 7).

Noncompressibility (Fig. 8) or intraluminal echogenicity are features of DVT that will likely be most evident during scanning for regional anesthesia. If suspicion exists that a thrombus is present, scanning with color Doppler may be helpful in identifying obstruction to or absent blood flow. The anesthesiologist must be mindful of the limitations and artifacts related to color Doppler.[1,2] Most importantly, the Doppler equation precludes the detection of blood flow when the angle of incidence of the ultrasound beam is 90 degrees.[1,2] Further, when analyzing low-velocity structures such as the superficial femoral vein, the velocity scale should be turned down. In the case provided (Fig. 7), the scale was set at 11 cm/sec to evaluate venous flow. In the case of the carotid artery, velocity scales will need to be set higher (30 cm/sec) to help prevent aliasing (see above).

Aneurysms

Excluding the aorta, the reported incidence of peripheral aneurysms in hospitalized patients is only 0.007%.[12,13] However, peripheral aneurysms most commonly occur in the popliteal artery as shown in Figure 9. The femoral artery, visualized when locating the femoral nerve, is less frequently involved with aneurismal disease. Aneurysms are saccular or spindle-shaped

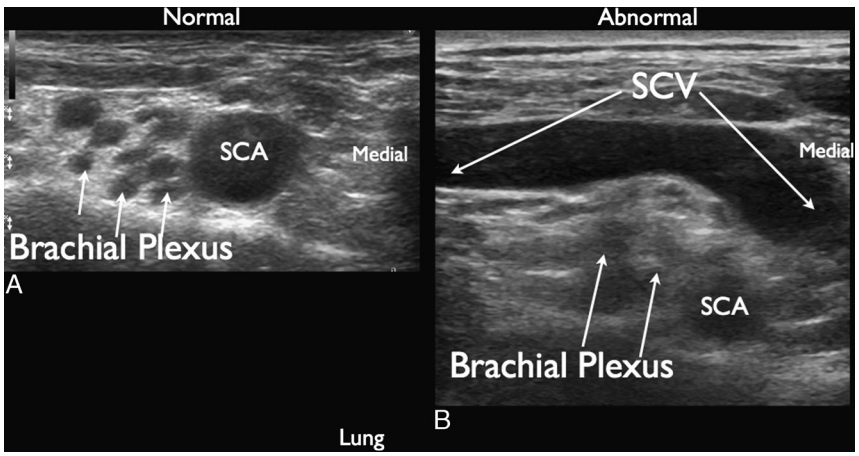

FIGURE 10. Elevated central venous pressure. A, Represents the normal situation in which the subclavian artery is the only visualized vascular structure during a supraclavicular block. B, Represents a dilated subclavian vein looping anterior to the supraclavicular brachial plexus and the subclavian artery. SCA indicates subclavian artery; SCV, subclavian vein. This lesion was identified while imaging for a supraclavicular nerve block. This lesion reflects elevated central venous pressure likely related to tricuspid regurgitation. Normally, the subclavian vein is not seen while imaging in the supraclavicular fossa for a brachial plexus block. Screen right in both images represents a medial/anterior direction.

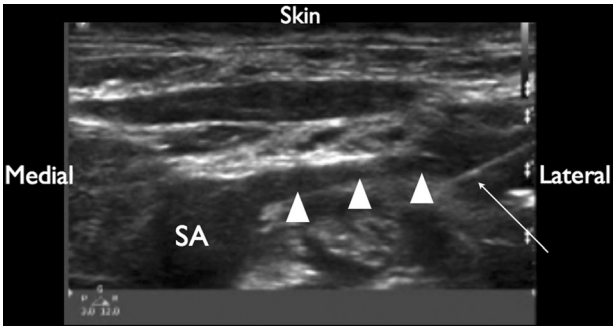

FIGURE 11. Unintentional puncture of a branch of the subclavian artery. The needle is seen through and through a structure believed to be the transverse cervical artery. This puncture resulted in a postsupraclavicular block hematoma that was controlled with compression. SA indicates subclavian artery, and the triangles mark the long-axis view of the transverse cervical artery. The arrow indicates the needle puncturing the transverse cervical artery.

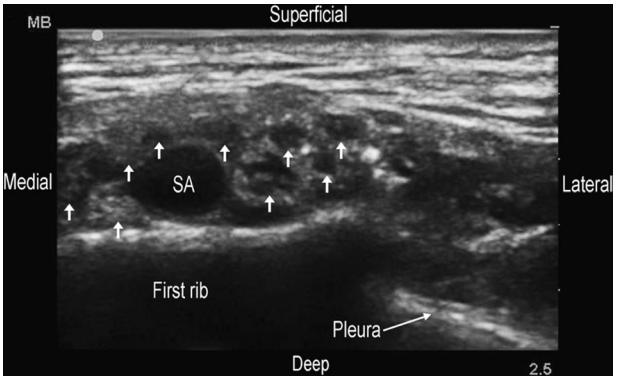

FIGURE 13. "Rainbow" arrangement of the supraclavicular brachial plexus. This is a short-axis image of the subclavian artery (SA), pleura, and the first rib. In this patient, the neural structures (likely the divisions and cords) are seen surrounding the subclavian artery in a rainbow-like fashion. That is, they are located on either side (medial and lateral) as well as superiorly. Arrows indicate the individual neural elements. Classically, the brachial plexus lies lateral to the subclavian artery (Fig. 10A). The authors believe that the appreciation and identification of such neural variation will likely improve the quality of the block.

dilatations of the vessel lumen. Ultrasound examination is the initial investigation of choice and can reveal information on diameter, as well as the presence of thrombosis. False or pseudoaneurysms occur in up to 4% of cases after percutaneous transluminal angioplasty.[14] Aneurysms can be differentiated from other perivascular hypoechoic structures such as hematoma, seroma, or lymphocele by the bidirectional "to and fro" flow through the neck of the aneurysm, as visualized best by color Doppler.[15]

Elevated Central Venous Pressure

The internal jugular vein is commonly imaged during brachial plexus blockade above the clavicle. Raised central venous pressure occurs in a variety of pathologic conditions and may be noticed in the internal jugular or even subclavian vein during an interscalene or supraclavicular block. Figure 10B is an example of a dilated subclavian vein that is looping anterior to the supraclavicular brachial plexus in a patient with tricuspid regurgitation, chronic right-sided heart failure, and elevated central venous pressure. Given that the transducer was positioned in the supraclavicular fossa, a supraclavicular nerve block would be technically challenging, with a higher risk of vessel puncture, hematoma formation, and possible intravascular injection. It should be noted that in the standard view for a supraclavicular block (as in this example), the subclavian vein is usually not visualized.

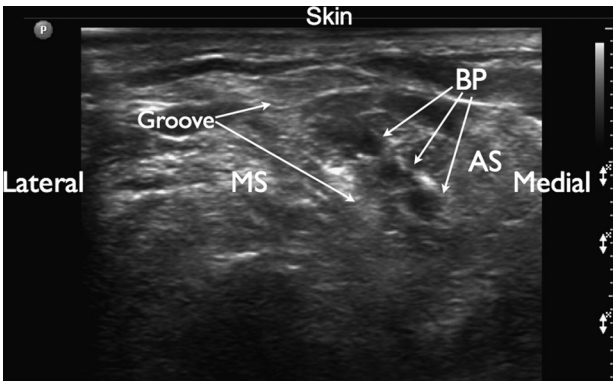

FIGURE 12. Atypical location of the brachial plexus. This image depicts the brachial plexus in the midneck crossing directly through the anterior scalene muscle. Notice that the "empty" interscalene groove is located just posteriolateral to the actual nerves. The anesthesiologist recognized this variant anatomy and performed the injection into the anterior scalene muscle. AS indicates anterior scalene muscle; BP, brachial plexus (roots); MS, middle scalene muscle.

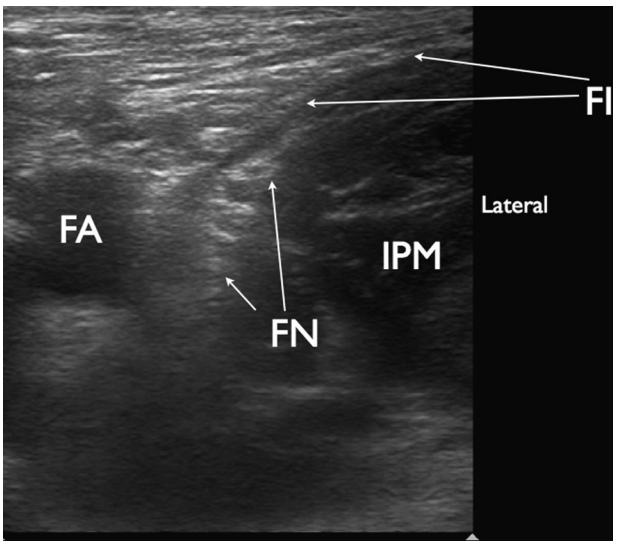

FIGURE 14. Atypical femoral nerve. This is a case of the femoral nerve that appears to be embedded in the iliopsoas muscle. Classically, the femoral nerve is an oval structure that is found under the fascia iliaca and adjacent to the iliopsoas muscle. It would be reasonable to conclude that an injection extramuscularly may result in a suboptimal block. FA indicates femoral artery; FI, fascia iliaca; FN, femoral nerve; IPM, iliopsoas muscle.

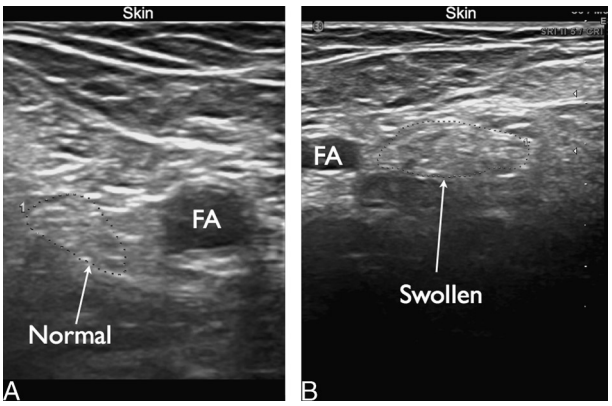

FIGURE 15. Femoral neuropathy. These are short-axis images of the infrainguinal femoral nerve that come from the same patient. A, Normal right-sided femoral nerve. B, Swollen and enlarged left femoral nerve. This patient sustained a dramatic femoral neuropathy after a total hip revision on the left side. The patient was having an ultrasound examination by a radiologist as part of a comprehensive diagnostic evaluation. The dotted line in each image outlines the femoral nerve as seen by the radiologist. The decision where to draw this line may seem arbitrary to some readers. However, the line was drawn based on the observed presence of a fascicular pattern (internal hypoechoic circles). This pattern is clearly evident within the tracing and absent adjacent to it.

Vascular Anatomy

It should be noted that normal anatomic variation in blood vessels can also create an obstacle to needle insertion and successful block placement. Examples of typical vascular variations that may impede typical needle approaches would include the dorsal scapular artery and the transverse cervical artery in the brachial plexus blocks above the clavicle. In the lower extremity, the lateral femoral circumflex artery can be a challenge to avoid during the performance of femoral nerve blocks. Figure 11 depicts an unintentional puncture of what is presumed to be a large transverse cervical artery during a supraclavicular block. This puncture resulted in a postprocedure hematoma that was controlled with compression. This case emphasizes the importance of conducting a prepuncture scan with color Doppler.

NERVES

Ultrasound can now rival magnetic resonance imaging as an imaging modality for peripheral nerves.[16] Nerves can be hypoechoic or hyperechoic depending on the nature of the surrounding tissue and the amount of connective tissue within the nerve itself.[17] Most often, a honeycomb pattern is evident in the short-axis view, with hypoechoic nerve fascicles surrounded by the echogenic epineurium.

A variety of relatively common pathologies such as hereditary neuropathies, nerve compression, nerve entrapment, rheumatologic disorders, infectious disorders, nerve tumors, intraneural ganglia, and anatomic variants may be encountered during the conduct of UGRA. If intrinsic or extrinsic nerve abnormalities are encountered, an alternative anesthetic management should be considered because neural pathology is a relative contraindication to nerve blockade.[18] Perioperative nerve injury is a complex and multifactorial process. The use of ultrasound guidance does not necessarily prevent or reduce the incidence of nerve injury.[19,20]

Anatomic Variants

Neural anatomic variants are commonplace, potentially undermining the success of UGRA. For example, the anatomy of the upper nerve roots of the brachial plexus is anomalous in 13% to 35% of cases.[21–23] Figure 12 demonstrates neural tissue directly penetrating the anterior scalene muscle of an 80-year-old man presenting for a rotator cuff repair. Of note, the interscalene groove has no neural tissue present and is easy to identify just posteriolateral to the anterior scalene muscle.

The resurgence in popularity of supraclavicular blockade and the recent description of the "corner-pocket" ultrasound-guided technique[24] rely on the normal location of the divisions of the brachial plexus immediately lateral to the subclavian artery and above the first rib. Anomalous nerve locations can compromise the success and safety of ultrasound-guided supraclavicular techniques (Fig. 13).[25] Variations in the anatomy of the cords and nerves relative to the axillary artery are also well recognized.[26]

Reports of anomalous nerve anatomy in the lower extremity are less common, possibly reflecting the scope of modern regional anesthetic practice. Nonetheless, Figure 14 demonstrates a case of what we believe to be the femoral nerve embedded in the iliopsoas muscle. Classically, the femoral nerve divides into the anterior and posterior divisions below the inguinal ligament.[27] Descriptions, however, do exist of this branching occurring more proximally, above the inguinal ligament.[28] In 1 cadaver study, psoas or iliacus muscle slips were noted to cover the femoral nerve in 7.9% of cases.[29]

Inflammatory Neuritis

Compressions by hematoma or trauma from a retractor are the most common causes of perioperative inflammatory neuritis, but other mechanisms include sepsis and intraoperative limb positioning. The incidence of femoral nerve palsy after total hip arthroplasty is less common than sciatic nerve injury, and this has been reported to be 0.7%.[30] Figure 15 depicts a femoral

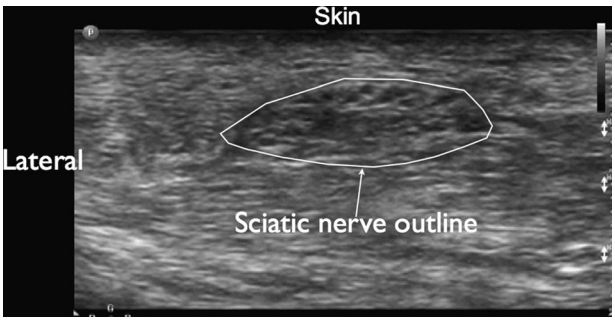

FIGURE 16. Swollen sciatic nerve. This is a short-axis image of an enlarged sciatic nerve with swollen fascicles in a patient with a diabetic peripheral neuropathy. The image was acquired approximately 5 cm proximal to the popliteal crease. The anesthetic plan for this patient was a combined sciatic and proximal saphenous nerve block to act as a surgical anesthetic for a below-the-knee guillotine amputation. The anesthesiologist recognized the abnormal nerve before the injection. However, given the potential morbidity of a general anesthetic (secondary to the patient's severe cardiopulmonary disease), the decision was made to proceed with the block. The decision where to draw the nerve outline is supported by the same process as described for Figure 15. In addition, the hypoechoic adipose tissue surrounding the sciatic nerve clearly demarcates the boarder of the neural tissue.

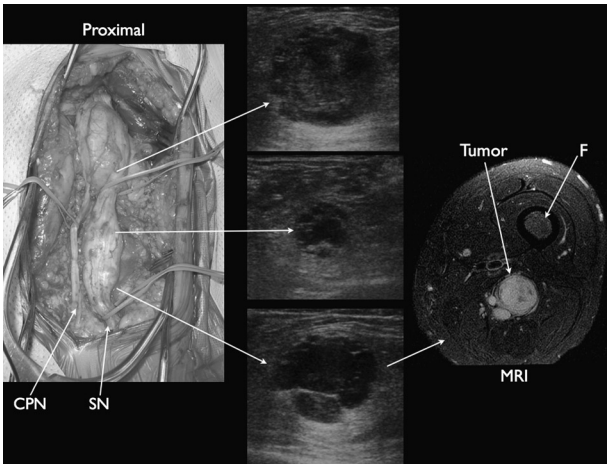

FIGURE 17. Schwannoma. This image displays the operative dissection of this large benign peripheral nerve tumor originating from the sciatic nerve. The corresponding short-axis ultrasound images and magnetic resonance image are provided as references. The tumor images are the large heterogeneous and mostly hypoechoic circles indicated by the arrows. In this particular case, the ultrasound examination was conducted intraoperatively to help assist the surgeons in making the most effective incision and to confirm that all the tumor was resected. F indicates femur.

nerve of a patient who developed a left-sided femoral nerve palsy after a total hip arthroplasty. The nerve appears swollen and enlarged, particularly when compared with the contralateral side. Postoperatively, the patient developed a dense motor deficit of the quadriceps muscle, as well as sensory loss in the anterior thigh and knee. It is important to note that this patient did not receive a femoral nerve block.

If an abnormality in the target nerve is suspected, scan the contralateral side as a control. If swelling or distorted architecture is identified, there is significant chance that the nerve is abnormal. Careful thought should be given to altering the anesthetic plan. Figure 16 demonstrates an enlarged sciatic nerve as imaged 5 cm proximal to the popliteal crease in a patient with diabetes with known peripheral neuropathy. In this image, swollen fascicles are noted with a grossly abnormal diameter. Given this patient's severe concomitant cardiopulmonary condition, a decision was made to still proceed with the nerve block as a surgical anesthetic for a below-the-knee amputation.

Nerve Tumors

Peripheral nerve tumors are infrequent in comparison with other primary neurologic tumors.[31,32] Indeed, malignant tumors have an incidence of only 0.1 per 100,000.[33] Both schwannomas and neurofibromas can be detected by ultrasound, although it is difficult to distinguish between these 2 pathologies.[34] In both cases, hypoechoic masses may be seen originating from the nerves, sometimes with posterior acoustic enhancement . Figure 17 represents a dramatic example of a large schwannoma originating from the sciatic nerve in the popliteal fossa. In this particular patient, the anesthesiologist was requested by the surgeons to help identify an incision site that would provide direct access to the middle of the tumor.

Neurofibromas can sometimes have hyperechoic tissue layers, which, when alternating with hypoechoic layers, create a "target" sign. Other masses such as hemangiomas, lymphomas, and ganglia may also develop inside nerves. Nonneural tumors may also invade peripheral nerves. Ultrasound can help to define its size and its relationship to the surrounding tissue and may also be used for needle-guided biopsy.[34]

Nerve Entrapment

Nerves are generally compressible and alter their shape depending on the volume of the anatomic space that they traverse. Although short periods of compression usually produce only a temporary neuropraxia, prolonged severe pressure can distort the nerve architecture. Extrinsic compression of a nerve may occur anywhere in the body. Nerve flattening, with fusiform swelling of the nerve proximal to the lesion, may be encountered on ultrasound imaging. In such entrapment neuropathies, the nerve may also become hypoechoic at and proximal to the compression site. This loss of echogenicity occurs because of swelling of the fascicles and decreased echogenicity of the epineurium.[35] Figure 18B demonstrates the lateral antebrachial cutaneous (LABC) nerve of a patient who presented with a neuropathic syndrome of his anterior lateral forearm. Lateral antebrachial cutaneous nerve entrapment is a diagnosis, which, in such circumstances, should be considered.[36] This patient was referred to one of the authors by a plastic surgeon, requesting a trial block of this nerve in the antecubital fossa. The goal was to diagnose a lesion at this level. By tracing distally from the musculocutaneous nerve in the axilla (Fig. 18A), the LABC was found. In the author's experience, the nerve appeared fusiform

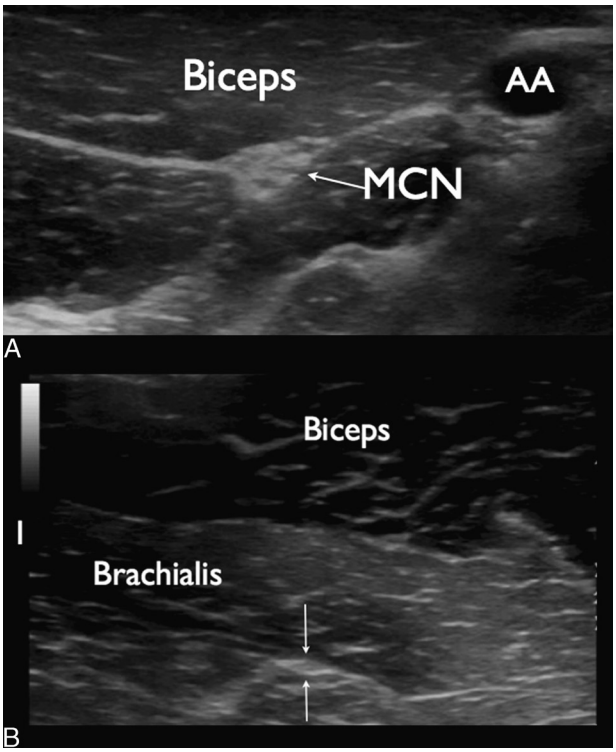

FIGURE 18. Lateral antecubital brachial cutaneous neuropathy. The patient was experiencing a chronic pain syndrome involving the entrapment of this the LABC nerve. A, High-resolution short-axis image of the musculocutaneous nerve (MCN) in the proximal arm. This nerve was followed distally until the LABC nerve was seen branching off. B, Arrows indicate the fusiform LABC nerve imaged approximately 2 cm proximal to the antecubital fossa. In the author's experience, this nerve appeared swollen and larger than expected.

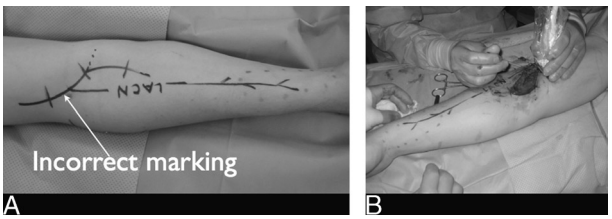

FIGURE 19. Operative dissection. A, Incorrect markings that the surgeons made before skin incision. The surgeons were unable to find the nerve using these surface landmarks. The LABC nerve was actually more medial. B, The anesthesiologists used ultrasound to identify the nerve and placed a 22-gauge spinal needle adjacent to it. The surgeons dissected along the needle and successfully found the LABC nerve.

and swollen. An injection of local anesthetic around the nerve resulted in relief of the neuropathic pain and so a decision was made to proceed to decompressive surgery. Intraoperatively, however, the surgeons could not find the LABC nerve. Therefore, under ultrasound guidance, a spinal needle was inserted next to the nerve (Fig. 19). With this guidance, the surgeons were able to dissect a small fascial band from the nerve. Postoperatively, the patient was pain-free.

In summary, part 1 examined common pathologic conditions affecting the tissues critically involved with UGRA: blood vessels and nerves. Part 2 will expand our discussion of sonopathology to include interesting cases associated with bone, viscera, subcutaneous tissue, and foreign bodies. As in part 1, we emphasize potential clinical connections to anesthesiologists practicing regional anesthesia.

ACKNOWLEDGMENTS

The authors thank Mr Liang Liang, BMSc, Research Fellow, Department of Anesthesia, Toronto Western Hospital, Toronto, for his assistance in formatting and editing of images during the preparation of the article.

REFERENCES

1. Sites B, Brull R, Chan V, et al. Part I of II: Artifacts and pitfall errors associated with ultrasound guided regional anesthesia: understanding the basic principles of ultrasound physics and machine operations. *Reg Anesth Pain Med*. 2007;32:412–418.
2. Sites B, Brull R, Chan V, et al. Part II of II: Artifacts and pitfall errors associated with ultrasound guided regional anesthesia: a pictorial approach to understanding and avoidance. *Reg Anesth Pain Med*. 2007;32:419–438.
3. Duggan E, Brull R, Lai J, Abbas S. Ultrasound guided brachial plexus block in a patient with multiple glomangiomatosis. *Reg Anesth Pain Med*. 2008;33:70–73.
4. Warlow C. Endarterectomy for asymptomatic carotid stenosis? *Lancet*. 1995;345:1254–1255.
5. Burkitt HG, Quick CR, Gatt DT. Vascular disorders. In: Burkitt HG, Quick CR, Gatt DT, eds. *Essential Surgery*. 2nd ed. Edinburgh, UK: Churchill Livingstone; 1996;453–500.
6. Tahmasebpour HR, Buckley AR, Cooperberg PL, Fix CH. Sonographic examination of the carotid arteries. *Radiographics*. 2005;25:1561–1575.
7. Sites BD, Spence BC, Gallagher JD, Beach ML. On the edge of the ultrasound screen: regional anesthesiologists diagnosing nonneural pathology. *Reg Anesth Pain Med*. 2006;31:555–562.
8. Geerts WH, Code KI, Jay RM, Chen E, Szalai JP. A prospective study of venous thromboembolism after major trauma. *N Engl J Med*. 1994;331:1601–1606.
9. Kerr TM, Cranley JJ, Johnson JR, et al. Analysis of 1084 consecutive lower extremities involved with acute venous thrombosis diagnosed by duplex scanning. *Surgery*. 1990;108:520–527.
10. Fraser JD, Anderson DR. Venous protocols, techniques, and interpretations of the upper and lower extremities. *Radiol Clin North Am*. 2004;42:279–296.
11. Sutin KM, Schneider C, Sandhu NS, Capan LM. Deep venous thrombosis revealed during ultrasound guided femoral nerve block. *Br J Anaesth*. 2005;94:247–248.
12. Guvendik L, Bloor K, Charlesworth D. Popliteal aneurysm: sinister harbinger of sudden catastrophe. *Br J Surg*. 1980;67:294–296.
13. Lawrence PF, Lorenzo-Rivero S, Lyon JL. The incidence of iliac, femoral, and popliteal artery aneurysms in hospitalized patients. *J Vasc Surg*. 1995;22:409–415.
14. Moll R, Habscheid W, Landwehr P. The frequency of false aneurysms of the femoral artery following heart catheterization and PTA (percutaneous transluminal angioplasty). *Rofo*. 1991; 154:23–27.
15. Sacks D, Robinson ML, Perlmutter GS. Femoral arterial injury following catheterization. Duplex evaluation. *J Ultrasound Med*. 1989;8:241–246.
16. Martinoli C, Bianchi S, Derchi LE. Tendon and nerve sonography. *Radiol Clin North Am*. 1999;37:691.
17. Sites BD, Brull R. Ultrasound guidance in peripheral regional anesthesia: philosophy, evidence-based medicine, and techniques. *Curr Opin Anaesthesiol*. 2006;19:630–639.
18. Neal JM, Bernards CM, Hadzic A, et al. ASRA practice advisory on neurologic complications in regional anesthesia and pain medicine. *Reg Anesth Pain Med*. 2008;33:404–415.
19. Hebl JR. Ultrasound guided regional anesthesia and the prevention of neurologic injury: fact or fiction? *Anesthesiology*. 2008;108: 186–188.
20. Koff MD, Cohen JA, McIntyre JJ, Carr CF, Sites BD. Severe brachial plexopathy after an ultrasound guided single-injection nerve block for total shoulder arthroplasty in a patient with multiple sclerosis. *Anesthesiology*. 2008;108:325–328.
21. Kessler J, Gray AT. Sonography of scalene muscle anomalies for brachial plexus block. *Reg Anesth Pain Med*. 2007;32:172–173.
22. Natsis K, Totlis T, Tsikaras P, Anastasopoulos N, Skandalakis P, Koebke J. Variations of the course of the upper trunk of the brachial plexus and their clinical significance for the thoracic outlet syndrome: a study on 93 cadavers. *Am Surg*. 2006;72:188–192.
23. Harry WG, Bennett JD, Guha SC. Scalene muscles and the brachial plexus: anatomical variations and their clinical significance. *Clin Anat*. 1997;10:250–252.
24. Soares LG, Brull R, Lai J, Chan VW. Eight ball, corner pocket: the optimal needle position for ultrasound guided supraclavicular block. *Reg Anesth Pain Med*. 2008;33:94–95.
25. Chin K, Niazi A, Chan VW. Brachial plexus anatomy in the supraclavicular region detected by ultrasound. *Anesth Analg*. 2008;107:729–731.
26. Pandey SK, Shukla VK. Anatomical variations of the cords of brachial plexus and the median nerve. *Clin Anat*. 2007;20:150–156.
27. Romanes GJ. The hip and thigh. In: Romanes GJ, ed. *Cunningham's Manual of Practical Anatomy*. Vol. 1. 15th ed. Oxford, UK: Oxford Medical Publications; 1992.
28. Das S, Vasudeva N. Anomalous higher branching pattern of the femoral nerve: a case report with clinical implications. *Acta Medica (Hradec Kralove)*. 2007;50:245–246.

29. Vazquez MT, Murillo J, Maranillo E, Parkin IG, Sanudo J. Femoral nerve entrapment: a new insight. *Clin Anat*. 2007;20:175–179.

30. Weber ER, Daube JR, Coventry MB. Peripheral neuropathies associated with total hip arthroplasty. *J Bone Joint Surg Am*. 1976;58:66–69.

31. Gruber H, Glodny B, Bendix N, Tzankov A, Peer S. High-resolution ultrasound of peripheral neurogenic tumors. *Eur Radiol*. 2007; 17:2880–2888.

32. Kehoe NJ, Reid RP, Semple JC. Solitary benign peripheral-nerve tumors. Review of 32 years' experience. *J Bone Joint Surg Br*. 1995;77:497–500.

33. Anghileri M, Miceli R, Fiore M, et al. Malignant peripheral nerve sheath tumors: prognostic factors and survival in a series of patients treated at a single institution. *Cancer*. 2006;107:1065–1074.

34. Reynolds DL Jr, Jacobson JA, Inampudi P, Jamadar DA, Ebrahim FS, Hayes CW. Sonographic characteristics of peripheral nerve sheath tumors. *AJR Am J Roentgenol*. 2004;182:741–744.

35. Martinoli C, Bianchi S, Pugliese F, et al. Sonography of entrapment neuropathies in the upper limb. *J Clin Ultrasound*. 2004;32:438–450.

36. Naam NH, Massoud HA. Painful entrapment of the lateral antebrachial cutaneous nerve at the elbow. *J Hand Surg Am*. 2004;29:1148–1153.

Clinical Sonopathology for the Regional Anesthesiologist

Part 2: Bone, Viscera, Subcutaneous Tissue, and Foreign Bodies

Brian D. Sites, MD, Alan J.R. Macfarlane, MBChB, MRCP, FRCA,† Vincent R. Sites, MD,‡ Ali M. Naraghi, MD, FRCR,§ Vincent W.S. Chan, MD, FRCPC,|| John G. Antonakakis, MD,¶ Mandeep Singh, MBBS, MD,|| and Richard Brull, MD, FRCPC||*

Abstract: The use of ultrasound to facilitate regional anesthesia is an evolving area of clinical, education, and research interests. As our community's experience grows, it has become evident that anesthesiologists performing "routine" ultrasound-guided blocks may very well be confronted with atypical or even pathologic anatomy. As an educational resource for anesthesiologists, the following articles present examples of common sonopathology that may be encountered during ultrasound-guided regional anesthesia. This present article describes sonopathology related to bone, viscera, and subcutaneous tissue.

(*Reg Anesth Pain Med* 2010;35: 281–289)

In part 2, we expand our presentation of sonopathology to include bone, viscera, subcutaneous tissue, and medicinal foreign bodies. As in part 1, we attempt to highlight clinical correlations that emphasize the relevance to anesthesiologists participating in ultrasound-guided regional anesthesia (UGRA).

BONE

Cervical Rib

A cervical rib is present in approximately 1 in 200 people. Thoracic outlet syndrome may occur when the brachial plexus (particularly the lower trunk), the subclavian artery, or the subclavian vein is compressed by a cervical rib as these structures pass through 1 of the 3 anatomic spaces that comprise the thoracic outlet.[1] Although plain x-ray, computed tomography, or magnetic resonance imaging is generally used to image the thoracic outlet, ultrasound can also detect a cervical rib. A cervical rib will most likely present incidentally as a superficial hyperechoic linear structure while imaging the divisions of the brachial plexus for a supraclavicular block. Dynamic Doppler imaging may be useful in measuring the extent of vascular obstruction on hyperabducting the arm, which is one factor precipitating symptoms.[2] The incidental detection of an accessory rib may also occur during an interscalene or a stellate ganglion block. Given that a dropout shadow is likely to occur inferior to the accessory bone, the image of the brachial plexus may be compromised if contained within this artifact. Typical sonographic views may be further altered if the neurovascular anatomy is distorted. For example, a cervical rib can fuse with the first rib and displace the subclavian artery anteriorly. Furthermore, fibrous bands, commonly associated with cervical ribs, can insert onto the rib and compress neural structures. Finally, the subclavian artery may actually pass above the cervical rib.[3] Figure 1 demonstrates a dramatic image of a cervical rib that was unexpectedly found during scanning of the supraclavicular fossa. Further questioning of this subject revealed a subtle neuropathic pain syndrome, which was not surprising given the physical distortion of the brachial plexus. The presence of a cervical rib should prompt consideration of alternatives in the block approach, such as choosing an infraclavicular block or modifying the needle approach.

Absent First Rib

The hyperechoic first rib and its dropout shadow provide useful landmarks during an ultrasound-guided supraclavicular block.[4] When the first rib is absent, then the pleura is fully visible underneath the artery, and both the comet tail sign and double-barreled subclavian artery artifacts may appear.[5] An ultrasound-guided supraclavicular block in such cases may be challenging, if not dangerous, because the first rib is not present to act as the typical "back stop" to prevent unintentional pleural puncture. Figure 2 is the supraclavicular region of a patient presenting for wrist surgery who had undergone a complete first rib resection 3 years previously. Of interest, this particular supraclavicular block was successful but had a slow onset, possibly because of the scar tissue impeding the spread of local anesthetic.

VISCERA

The thyroid gland is seen often and in significant detail when performing interscalene and stellate ganglion blocks. The anesthesiologists may be the first to identify incidental thyroid lesions.

Thyroid Nodules

Thyroid nodules (Fig. 3) occur in up to 50% of the population.[6] Ultrasound is the diagnostic imaging modality of choice for thyroid nodules. The thyroid has 2 lobes connected by an isthmus. Although up to 30% of people have an extra (pyramidal) lobe, this is rarely seen on ultrasound. Ultrasound scanning reveals the thyroid parenchyma to be a fine, homogeneous, hyperechoic structure compared with the adjacent muscles. Diffuse thyroid diseases such as Grave disease or Hashimoto thyroiditis (Fig. 4) alter the appearance of the parenchymal tissue, producing more subtle changes that may be challenging to detect. Surrounding the parenchyma is the echogenic thyroid capsule. Posterior to the gland is the hypoechoic air space inside the trachea, which is recognizable by interspaced distinct hyperechoic cartilaginous rings.

From the *Department of Anesthesiology, Dartmouth-Hitchcock Medical Center, Lebanon, NH; †Department of Anaesthesia, Glasgow Royal Infirmary, Scotland, UK; ‡Department of Radiology, Lahey Clinic, Burlington, MA; §Joint Department of Medical Imaging of University Health Network and Mount Sinai Hospital, Toronto Western Hospital, Toronto, Ontario, Canada; ||Department of Anesthesia and Pain Management, Toronto Western Hospital, University Health Network, Toronto, Ontario, Canada; and ¶Department of Anesthesiology, University of Virginia, Charlottesville, VA.

Accepted for publication August 14, 2009.

Address correspondence to: Richard Brull, MD, FRCPC, Department of Anesthesia and Pain Management, Toronto Western Hospital, 399 Bathurst St, Toronto, Ontario, Canada M5T 2S8 (e-mail: richard.brull@uhn.on.ca).

The authors did not receive funding for this study and have no conflict of interest to declare.

ISSN: 1098-7339
DOI: 10.1097/AAP.0b013e3181ddd21f

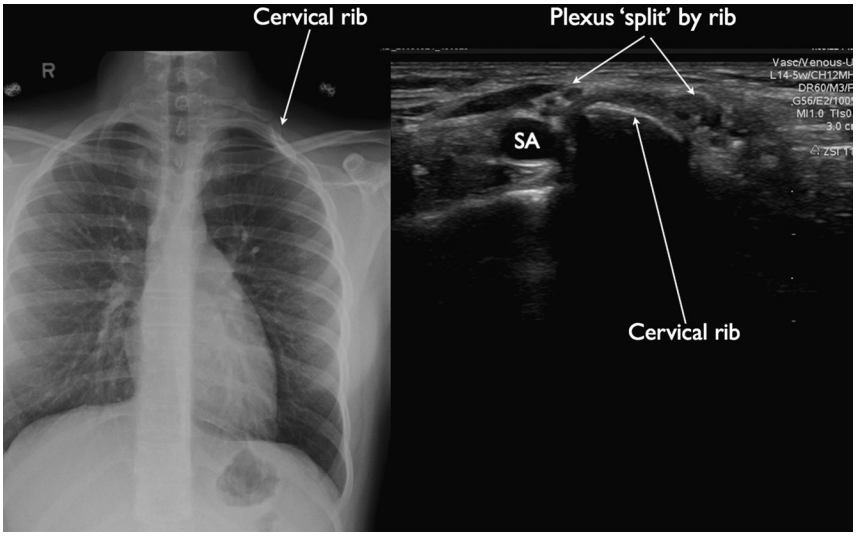

FIGURE 1. Cervical rib. This accessory bone was identified during scanning for a supraclavicular brachial plexus block. Identification of the accessory bone allowed the operator to guide the needle over the bone and into the brachial plexus. SA indicates subclavian artery; BP, brachial plexus.

For trained diagnostic sonographers, it can be challenging to distinguish between benign and malignant nodules based on sonographic features alone.[7] Although microcalcifications (punctuate echogenic spots without posterior acoustic shadowing), lack of hypoechoic "halo" (seen around most benign nodes), irregular margins, hypoechogenicity, and increased intranodular flow may all raise suspicion, no one is pathognomonic for malignancy. In combination, however, the likelihood of malignancy is increased. The number and size of nodules are nonspecific characteristics of malignancy, whereas lymphadenopathy and local invasion of adjacent structures are highly specific features of thyroid malignancy but are far less commonly seen.

Thyroid nodules may be encountered during the performance of an ultrasound-guided interscalene, cervical plexus, or facet blocks. If an incidental thyroid lesion is encountered during routine scanning for a peripheral nerve block, further consultation should be requested. The presence of a thyroid lesion(s), without clinical signs of hyperthyroidism or hypothyroidism, is unlikely to change the anesthetic management.

Lung: Pneumothorax

The pleura is identified as a linear and hyperechoic structure that slides during respiration. The comet tail sign is a useful artifact generated by multiple beam reverberations emanating

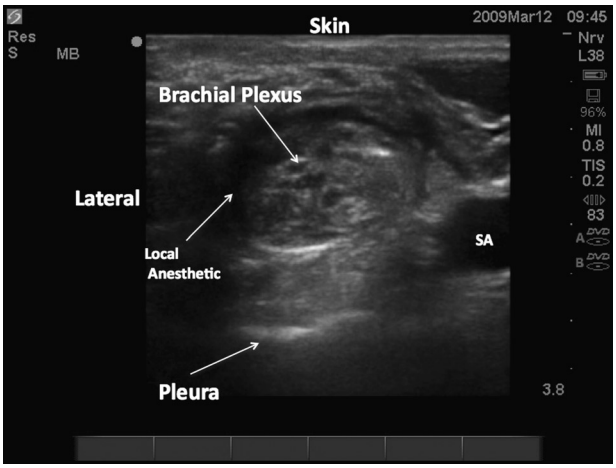

FIGURE 2. Ultrasound-guided supraclavicular brachial plexus nerve block in a patient with an absent first rib. The pleura is evident; however, no first rib was identified. In this image, the labeled hyperechoic line is the pleura. Normally, this would be the location to image the first rib. Dynamically, under real-time ultrasound, one could appreciate the sliding of the pleura at this labeled location.

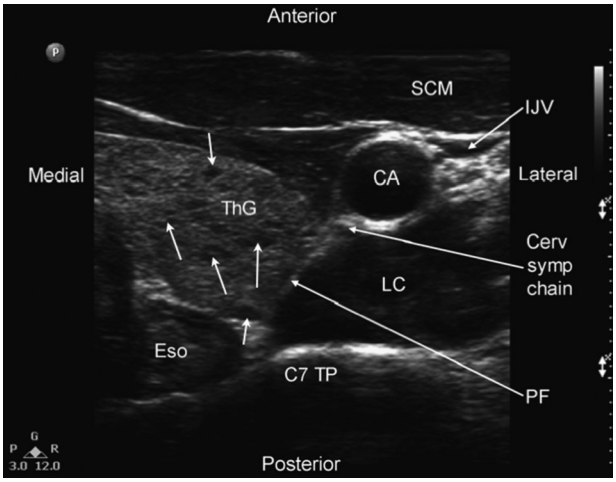

FIGURE 3. Thyroid nodules. This is a case where a multinodular thyroid was found during the performance of a stellate ganglion block. Figure 4 is a short-axis image at the level of the C7 showing multiple hypoechoic nodules (unlabeled arrows) in the thyroid gland parenchyma. Ultrasound-guided stellate ganglion blocks necessitate the deposition of local anesthetic at the level of the cervical sympathetic chain which usually lies posterior or posteromedial to the carotid artery (CA) and anterior to the prevertebral fascia (PF) covering the anterior border of longus colli muscle (LC). C7TP indicates transverse process of the C7 vertebral body; Cerv symp, cervical sympathetic chain; Eso, esophagus; IJV, internal jugular vein; SCM, sternocleidomastoid muscle; ThG, thyroid gland.

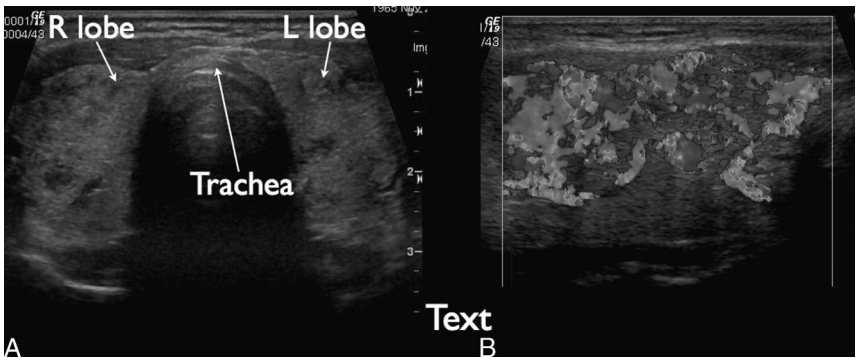

FIGURE 4. Hashimoto thyroiditis. These images come from a patient with tachycardia and hypertension. A, Short-axis view at the level of the thyroid isthmus. Both lobes of the thyroid gland are heterogeneous in echogenicity and contain hypoechoic nodules. B, Right lobe demonstrating the increased vascularity consistent with thyroiditis. Of note, the patient's diagnosis of Hashimoto thyroiditis was confirmed by biopsy.

from the pleura, which acts as a strong specular reflector.[8] Another important sign is the lung sliding sign, which is generated by the real-time countermovements of the visceral and parietal pleurae.

Pneumothorax is a potential complication of brachial plexus,[9] paraverterbral,[10] and intercostal nerve blocks.[11] Pneumothorax can be diagnosed by ultrasound, and it is already being incorporated in the focused abdominal sonography for trauma scan in some emergency centers.[12] One important presenting feature of a pneumothorax is the loss of the lung sliding sign. The analysis for a pneumothorax is best accomplished with M-mode ultrasound. M-mode (Motion) is the diagnostic ultrasound presentation of the temporal changes in echoes in which the depth of the echo-producing interfaces is displayed along one axis and time is displayed along the second axis, recording motion of the interfaces toward and away from the transducer. This is, in essence, B-mode ultrasound presented over time. M-mode was the first display used, and this continues to be useful for the precise timing of cardiac valve opening and correlating valve motion with electrocardiography, phonocardiography, and Doppler echocardiography. In comparison to real-time 2-dimensional ultrasound, M-mode offers a higher frame rate, which is the reason why it is useful for the evaluation of moving structures. The hallmark sign of a pneumothorax is the visualization of the M-mode "stratosphere" sign, indicating the absence of pleural sliding (Fig. 5A). The "seashore sign" (Fig. 5B) confirms pleural sliding and no pneumothorax.[13]

It is good practice to image the lung during ultrasound-guided supraclavicular, infraclavicular, intercostal, and paravertebral blocks to note the distance of the pleura relative to the proposed needle trajectory as well as to avoid pleural puncture in real-time. Lung sliding may be absent in patients without a pneumothorax but have lung fibrosis, scarring, or adult respiratory distress syndrome. Comet tail artifacts should be distinguished from other artifacts such as "horizontal artifacts." These are internal reverberation artifacts that do not spread to the bottom of the image as comet tail artifacts do. In subcutaneous emphysema, reverberation artifacts are also seen, but these are generated above the pleural line, which can make visualization of the pleura difficult, if not impossible.

Bowel: Hernia

Intestinal hernias are focal protrusions of tissue through fascial defects. Ten percent of the population will develop a hernia in their lifetime, 70% of which are inguinal.[14] Femoral hernias are visible medial to the femoral vein below the inguinal

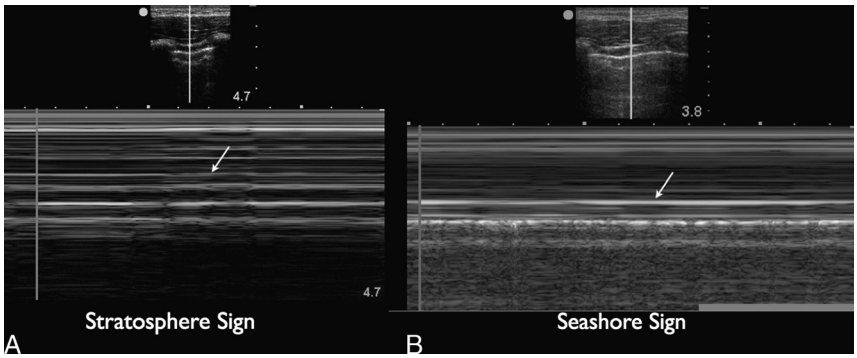

FIGURE 5. Pneumothorax and normal lung. A, ''Stratosphere sign.'' This image was generated by placing the transducer in the midclavicular line over ribs 2 and 3 and scanning with M-mode. In the case of pneumothorax, and thus absent pleural sliding, horizontal lines are visualized throughout, representing a laminar pattern (stratosphere sign) both above and beyond the pleural line (white arrow). B, ''Seashore sign.'' This is a M-mode ultrasound image in a patient without a pneumothorax. The pleural line is once again indicated by the white arrow, and above it, the motionless parietal structures are localized first. Below the pleural line, lung sliding appears as a homogenous granular pattern, showing a laminar pattern above pleural line (stationary chest wall) and granular appearance (seashore sign) deep into the pleural line, representing pleural sliding. (Images courtesy of Dr. Michael B. Stone, Department of Emergency Medicine, Kings County Hospital Center/SUNY Downstate, Brooklyn, NY.)

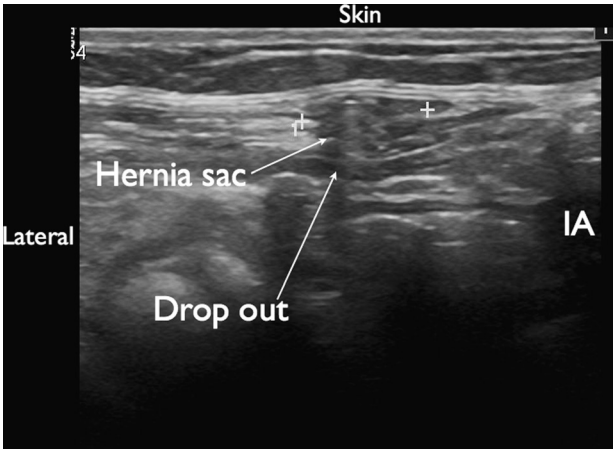

FIGURE 6. Inguinal hernia. This is a short-axis image of the region just proximal the inguinal ligament. Evident in this picture is a hypoechoic circular structure penetrating deeper through the tissue into the subcutaneous region. This structure is a hernia sac consisting of bowel contents. On dynamic ultrasound imaging, the radiologist could see peristalsis in this sac. The plus signs represent the calipers used for measuring. IA indicates iliac artery. The dropout shadow once again is a helpful clue to potential pathology. This image was obtained 1 cm proximal (suprainguinal) to where a femoral nerve block would normally be conducted. It is conceivable that hernia sacs could be present infrainguinally as well.

ligament, whereas inguinal hernias are located more cephalad. A variety of structures may herniate through the fascial defect including the soft tissue, the peritoneal sac, or the intestines (Fig. 6). Compared with other imaging modalities, real-time ultrasound has the advantage of allowing dynamic examination of hernias during the Valsalva maneuver.[15] Ultrasound may also help differentiate indirect from direct inguinal hernias by identifying the inferior epigastric artery. Herniated bowel contents may show peristalsis, with herniated adipose tissue appearing distinctly hyperechoic. Figure 7 demonstrates a hernia in the midline developing below the umbilicus. Bowel is clearly seen adherent to the linea alba.

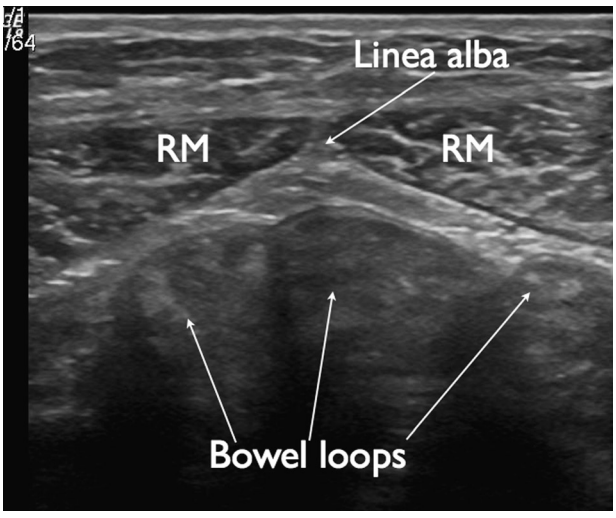

FIGURE 7. The beginnings of a midline hernia. This is a short-axis image just below the umbilicus. Note the linea alba that marks the midline. The bowel loops are easy to appreciate adherent to the posterior rectus sheath. RM indicates rectus muscle.

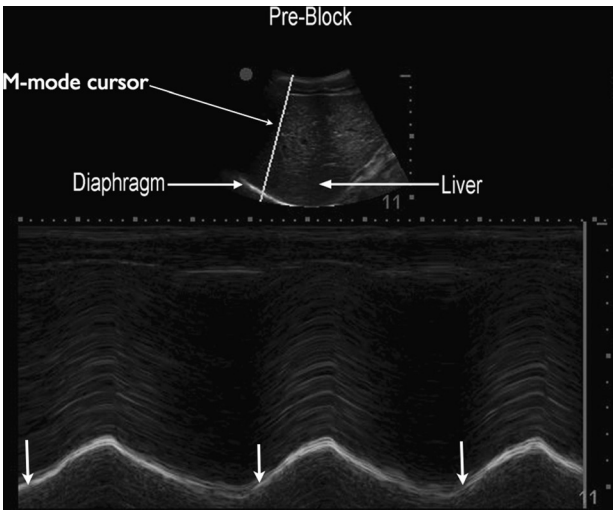

FIGURE 8. Normal breathing. This is an M-mode image through the liver with the transducer placed in the midaxillary line below the diaphragm. The M-mode cursor can be seen bisecting the diaphragm (image top). The M-mode image is seen at the bottom of the figure. This image is consistent with the normal diaphragmatic excursion pattern during tidal volume breathing. White arrows indicate the start of an inspiratory effort. The normal diaphragmatic breathing pattern is caudad movement of the diaphragm. This results in movement of the diaphragm line more superficially on the screen because it represents movement of the diaphragm toward the transducer.

Hernias would most likely be identified during the performance of a femoral, obturator, rectus sheath, transversus abdominus plane,[16] or ilioinguinal nerve block. It is conceivable that hernia contents could be damaged by needle advancement. If a hernia is suspected (previous multiple surgeries or history), increase the depth and search for the peritoneum and peristaltic

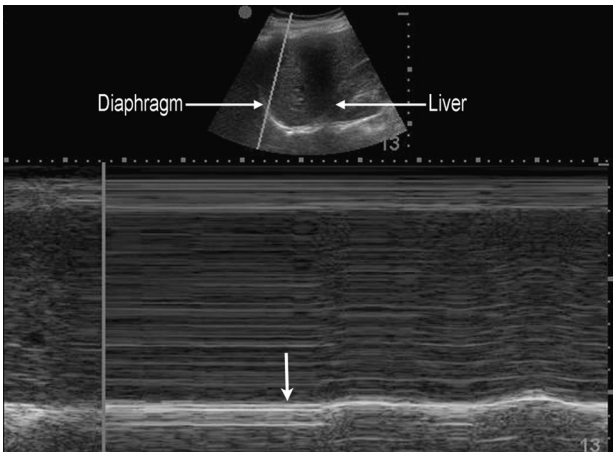

FIGURE 9. Impaired diaphragm. This is the same patient as in Figure 9, except 20 mins after an interscalene block. The diaphragmatic paralysis is evident, with demonstrable qualitative diminution in the magnitude of diaphragmatic excursions. The white arrow indicates the static diaphragm despite breathing. (Images courtesy of Dr. Sheila Riazi, Department of Anesthesia, Toronto Western Hospital, University of Toronto, Toronto, Ontario, Canada.)

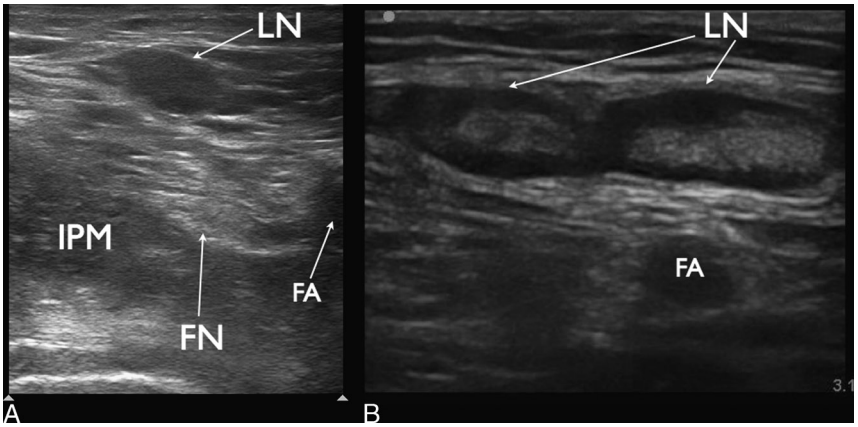

FIGURE 10. Femoral lymphadenopathy noted during a femoral nerve ultrasound scanning. Notice that lymph nodes have different appearances. Figure 11A demonstrates a hypoechoic structure; whereas Figure 11B reveals a heterogeneous structure. FA indicates femoral artery; FN, femoral nerve; IPM, iliopsoas muscle; LN, lymph node.

motion of bowel before needle insertion. As an example, the operator may choose not to perform a rectus sheath block (Fig. 7) in favor of a more lateral transversus abdominus plane block.

Diaphragm

Ultrasound enables the assessment of diaphragmatic movement through the use of M-mode ultrasound.[17] Figures 8 and 9 demonstrate a patient who was scanned before and shortly after completing a right interscalene nerve block. One can clearly appreciate the dramatic absence of diaphragmatic excursion.

Preblock scanning of the contralateral diaphragm in patients with a history of a spinal cord injury or phrenic nerve palsy may be helpful in formulating a final anesthetic plan when considering an interscalene or supraclavicular block. If the M-mode reveals contralateral diaphragmatic pathology, then consideration should be made to performing another block or aborting the procedure entirely.

SUBCUTANEOUS TISSUES

High-frequency ultrasound transducers commonly used during superficial nerve blockade enable the identification of a variety of pathologic structures. Ultrasound examination of the subcutaneous tissue involves dynamic application of different degrees of transducer pressure, finger palpation, and manual mobilization of the skin to help distinguish among masses, fluid collections, and fibrosis. Normal subcutaneous tissue is visualized on ultrasound as a discrete layer, characterized by a hypoechoic background of adipose tissue, with interpositioned linear echoes generated by the connective septa. Subcutaneous veins may be seen as elongated or rounded anechoic structures that run inside the larger septa that collapse with transducer pressure. Small sensory nerves may be seen coursing alongside the superficial veins, usually in the deep subcutaneous tissue. Lymphatics, which are also contained within the connective septae, are not typically visualized with ultrasound unless distended by fluid as in the case of subcutaneous edema.

Lymphadenopathy

Normal lymph nodes appear as flattened oval structures with a thin hypoechoic cortex and an echogenic, hypovascular hilum. Ultrasound is useful for imaging superficial nodes such

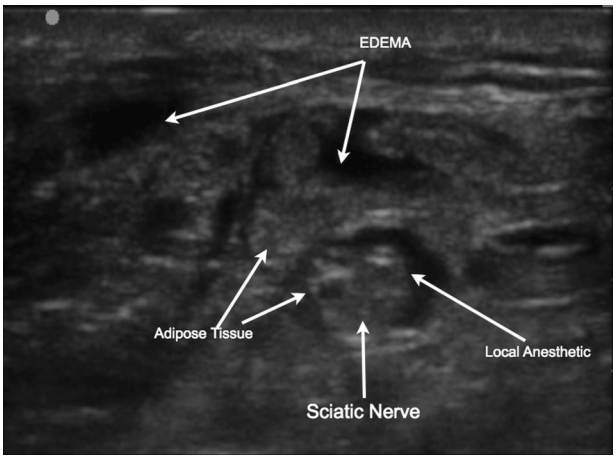

FIGURE 11. Popliteal fossa during the performance of a popliteal sciatic nerve block in a patient with chronic lower extremity edema. Notice the fat lobules becoming individual structures separated from each other by edema.

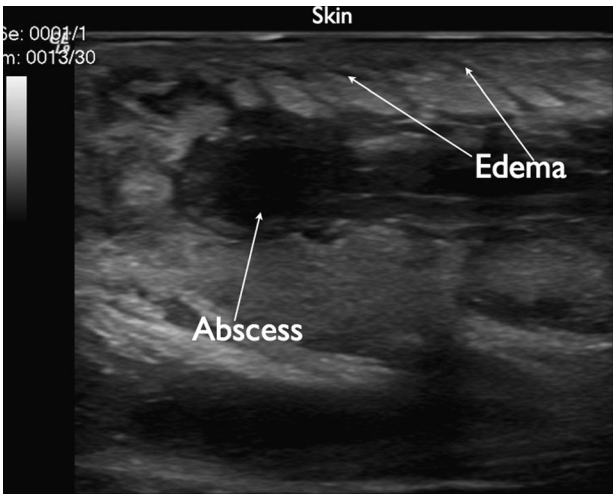

FIGURE 12. Abscess in an intravenous drug user. This is a short-axis image of the antecubital fossa in a patient with point tenderness and fever. The abscess appears as an irregular hypoechoic structure with variable echogenic areas representing purulent debris. Also evident in this image is superficial edema as previously described.

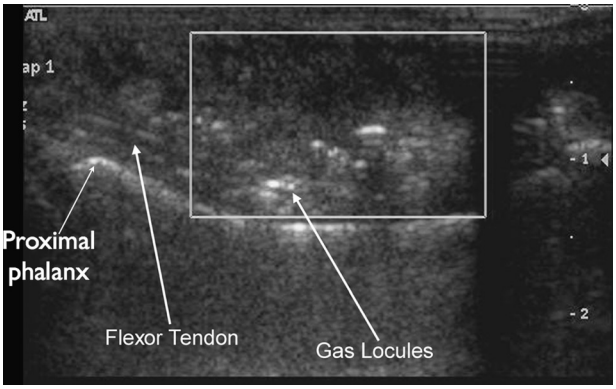

FIGURE 13. Tendon sheath gas. This is a long-axis ultrasound image through the volar aspect of the proximal phalanx of hand, showing echogenic locules (hyperechoic dots) of gas surrounding the flexor tendon. The proximal phalanx is seen posterior as a bright hyperechoic line, associated with an acoustic shadow.

as those in the cervical, inguinal, or axillary areas. Ultrasound is superior to palpation alone in detecting lymphadenopathy.[18] Although sonographic features can help differentiate malignant from benign nodes, the combination with fine-needle aspiration increases the sensitivity and specificity.[19] Enlarged nodes may be benign or malignant, so nodal size alone is not a reliable method for characterizing lymph nodes. The ultrasound characteristics of malignant infiltration include enlarged nodes that are usually rounded and show peripheral or mixed vascularity. They may have thickened outer wall, internal echoes, cystic formations, internal nodularity, and septations.[20] Finally, malignant nodes are usually noncompressible.

The anesthesiologist performing axillary, femoral, or interscalene nerve blocks will commonly image lymph nodes.

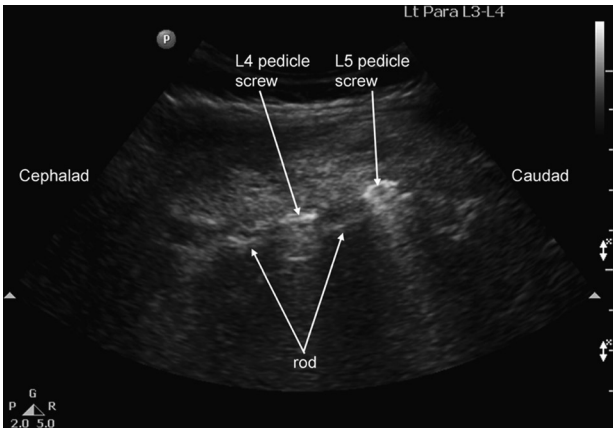

FIGURE 14. Spinal hardware. This longitudinal parasagittal image of the lumbar sacral spine was generated by placing the transducer in a ''paramedian'' location. This patient had a previous history of back surgery (laminectomy, decompression, and fusion of L3-5 levels). The ultrasound examination was performed before administration of a spinal anesthetic. The metallic hardware is visualized as hyperechoic lines, with the pedicle screws seen more superficial to the Harrington rods. The ligamentum flavum or the thecal sac is not seen in this view, suggesting possible difficulty in performance of a spinal anesthetic via a paramedian technique. (Image courtesy of Dr. Ki Jinn Chin, Department of Anesthesia, Toronto Western Hospital, University of Toronto, Toronto, Ontario, Canada.)

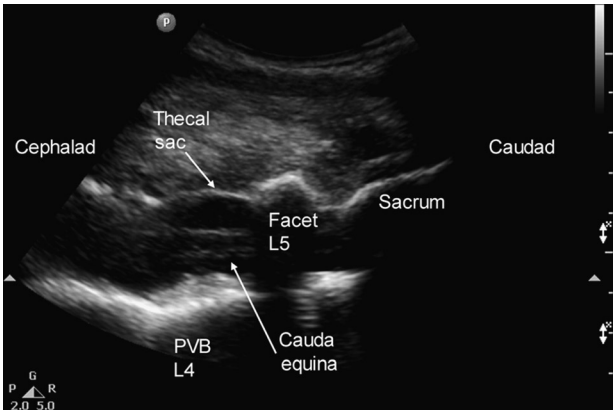

FIGURE 15. Postlaminectomy long-axis parasagittal image of the lumbar sacral spine. The absence of the saw-tooth pattern of the lamina and the distinct appearance of the thecal sac and cauda-equina at the level of the L4-5 interspace suggested ease of access to the subarachnoid space. The spinal anesthetic was performed without difficulty in this patient. PVB L4 indicates posterior part of vertebral body of L4 vertebra.

In the axilla, lymph nodes often have a similar appearance as nerves and can potentially confuse the operator. In the inguinal region, lymph nodes are commonly encountered in the context of performing femoral nerve blocks (Fig. 10). Anesthetic management in the patient depicted in Figure 10A was changed empirically from a continuous femoral catheter to a single-shot injection to reduce the possibility of infection. Femoral catheters appear to be at particular risk of colonization compared with other locations.[21] Although guidelines exist on minimizing the risk of infection during placement of continuous catheters,[22] it remains unclear whether an indwelling continuous

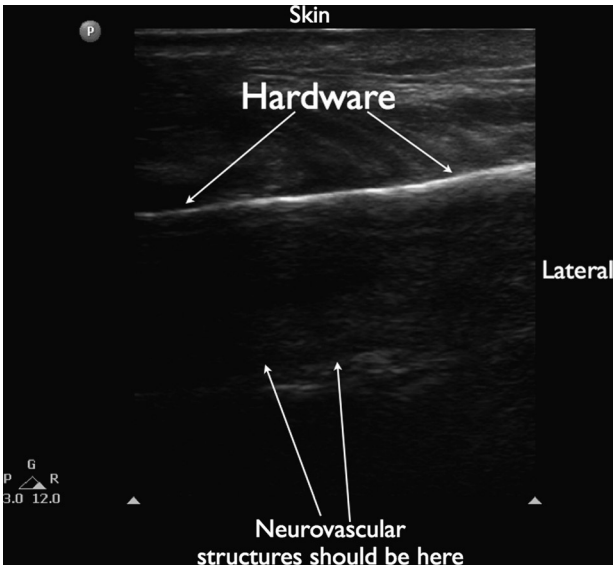

FIGURE 16. Clavicle hardware. The transducer was held in the supraclavicular fossa as standard for a supraclavicular block. The hardware extended into the supraclavicular space, impeding the penetration of the ultrasound beam. The creation of a dropout shadow effectively prevented the visualization of the neural and vascular structures. A decision was made by the anesthetic team to perform a different nerve block.

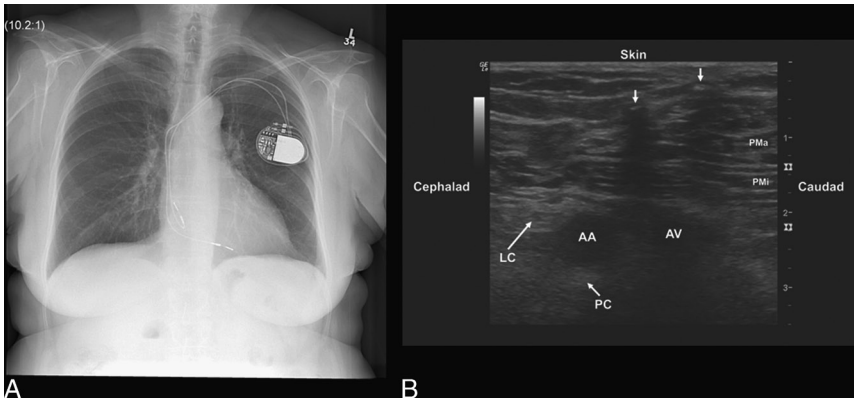

FIGURE 17. Permanent cardiac pacemaker. A, Chest radiograph of a 70-year-old woman scheduled for a wrist arthrodesis and first metacarpophalangeal joint arthroscopy of the left hand. A pacemaker (DDD) had been inserted 3 years previously for symptomatic syncope and third-degree heart block. B, Preprocedure systematic sonographic survey revealed 2 pacemaker leads (small white arrows) as 2 distinct bright hyperechoic dots with pronounced dropout shadows posteriorly. The acoustic shadow of the pacemaker wires obscured the appearance of the medial cord that lies between the axillary artery (AA) and the axillary vein (AV). The lateral (LC) and posterior cords (PC) could be visualized. A supraclavicular approach to the brachial plexus using ultrasound guidance alone was performed successfully without adverse sequelae. PMa indicates pectoralis major muscle; PMi, pectoralis minor muscle.

perineural catheter is appropriate in patients with documented lymphadenopathy.

Edema

Edema has a variety of causes, and this will inevitably be encountered by anesthesiologists participating in UGRA. In the early stages, edematous changes tend to involve the deep layer of the subcutaneous tissue. This is visualized on ultrasound as hypoechoic areas of fluid accumulation, whereas the most superficial layers of the subcutaneous tissue remain normal. As fluid accumulates, the connective septa enlarge and become anechoic strands caused by distension of the superficial network of lymphatic channels. As seen in Figure 11, fat lobules ultimately become individualized structures separated from one another by fluid. Edema may interfere with peripheral nerve blockade by distorting the neural anatomy, increasing the depth, masking hypoechoic structures, diluting local anesthetic injection, and possibly altering nerve stimulation thresholds. Conversely, hypoechoic fluid may actually facilitate imaging of the hyperechoic nerve by effectively outlining the target.

Abscess

The anesthesiologist may be one of the first members of the care team to identify a loculated fluid collection in a patient presenting for anesthesia. Ultrasound can facilitate differentiating between an abscess and cellulitis by demonstrating the spread of infection into deeper skin layers as well as into tendons, muscle, or joints. Cellulitis is visualized as an irregular, ill-defined hyperechoic appearance of fat with blurring of tissue planes, progressing to hypoechoic strands reflecting edema.[23] This pattern can be difficult to distinguish from simple edema. Figure 12 demonstrates a subcutaneous abscess that was noted in an intravenous drug user who presented for drainage. Abscesses are characteristically irregular fluid-filled hypoechoic areas with posterior acoustic enhancement, containing a variable amount of echogenic debris that represents purulent material. In highly echogenic collections, pressure with the transducer may cause fluctuation of the particles, which can help confirm the liquid nature of the mass. The formation of gas is possible in advanced disease or with gas-forming organisms such as *Clostridium*. The presence of gas may be suggested by scattered bright foci in the tissues (Fig. 13). The presence of an abscess near a nerve would likely preclude the placement of a continuous catheter and possibly even a single injection.

FOREIGN BODIES AND HARDWARE

Ultrasound is an excellent tool for detecting and evaluating foreign bodies. Unlike plain radiography, it can accurately determine the relationship of the foreign body to surrounding soft tissue structures.[24] Foreign bodies may be present in the subcutaneous tissues as the result of traumatic injuries or therapeutic procedures. We will focus on foreign bodies placed medicinally because they have the most relevance to UGRA.

Spinal Hardware

The role of ultrasound in central neuraxial procedures has been slower to develop because structures of interest lie relatively deep and are encased in bone, with only narrow acoustic windows available for imaging. Despite these limitations, ultrasound can provide prepuncture information on the appropriate spinal interspace and depth of the various targets.[25,26] Scanning the spine in both midline short-axis and paramedian long-axis

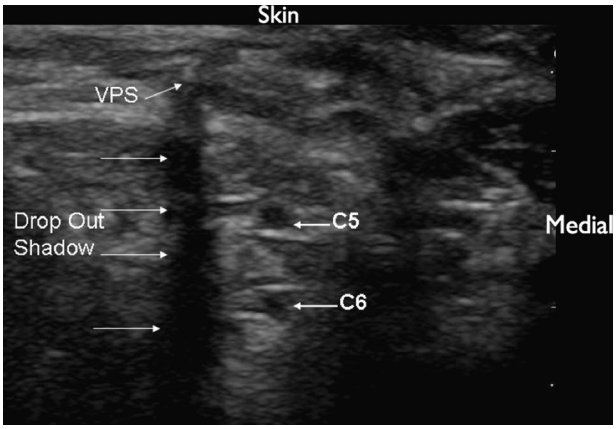

FIGURE 18. Ultrasound image of the C5-6 nerve roots during an interscalene brachial plexus imaging. The distinct dropout shadow was created by the high acoustic impedance of a ventricular-peritoneal shunt (VPS). In this particular case, the anesthesiologists did not know that the patient had a VPS.

(parasagittal) can reveal clinically relevant information such as the bony laminae, facet joints, ligamentum flavum, dura mater, and intrathecal space.[27] Evidence of previous spine surgery, such as laminectomy or insertion of spinal hardware, can be encountered during ultrasound-guided neuraxial blockade. Ultrasound waves cannot penetrate through metal (high acoustic impedance), thus generating prototypical anechoic dropout shadows. These artifacts effectively blanket all structures lying deep to the metal. This is particularly evident in parasagittal view of the lumbar spine depicted in Figure 14. In contrast, when bone is removed, such as in postlaminectomy patients,[28] detailed imaging of the spinal structures is possible (Fig. 15).

Clavicle Hardware

The clavicle is a common location for operative interventions. Figure 16 originates from a patient in whom a supraclavicular block was being considered. In this image, the edge of the clavicular hardware effectively prevented the ability to image the typical structures of the supraclavicular fossa. This procedure was aborted.

Tubes and Drains

There are an endless number of medical devices that may present themselves in the context of performing regional anesthesia. More common devices would include pacemaker wires (Fig. 17), pacemaker generators, vascular grafts, prosthetic material, chest tubes, and ventricular-peritoneal shunts (Fig. 18). Although a thorough history and physical is arguably the best way to identify potential objects that could complicate a nerve block, the anesthesiologist may be initially confronted with a foreign object during preprocedure scanning for a planned regional anesthetic. Figure 18 comes from a patient undergoing an interscalene nerve block. A small hyperechoic circle was seen with a distinct acoustic dropout shadow. On further questioning of the patient, it was discovered that the patient had a ventricular-peritoneal shunt. Given the proximity of the shunt to the brachial plexus, the nerve block was aborted.

CONCLUSIONS AND SCOPE OF PRACTICE ISSUES

Nerves and the tissues surrounding the nerves are commonly involved with pathology and/or atypical anatomy. The anesthesiologist will inevitably encounter some of these situations during the conduct of UGRA. This library of images and descriptions of sonopathology will hopefully add to the background knowledge and educational resources available to anesthesiologists. The incidental pathologic findings also create a management dilemma for the anesthesiologist, which is beyond the scope of this review but includes the assumption of responsibility for timely referral and comprehensive investigation, as well as ensuring definitive diagnosis by a radiologist or appropriate specialist.

It is our opinion that the appropriate behavior surrounding ultrasound findings should be no different from this traditional approach to the preanesthetic history and physical examination. Further relevant analogies between an appropriate ultrasound scope of practice and a traditional anesthetic practice would include the discovery of a vocal cord lesion during direct laryngoscopy, the discovery of an unexpected lesion on chest x-ray, or the identification of a complex cardiac rhythm. In these situations, documentation of the findings would be made, and consultation with an appropriate specialist would occur. It is our hope that an understanding and appreciation of sonopathology will help support the adjustment of anesthetic technique as indicated by the particular clinical scenario and initiate an early and appropriate consultation after surgery.

In summary, the continuing popularity of ultrasound will also undoubtedly foster the anesthesiologist's role as the perioperative physician. As anesthesiologists become increasingly familiar with ultrasound technology and sonographic anatomy, inevitably we will begin investigating our own patients at the point-of-care, detecting incidental occult pathology, and call on to assist our surgical colleagues in the operating room and beyond. We are nonetheless hopeful that this review will broaden the awareness of common sonopathology such that ultrasound can be used most effectively to advance knowledge and skills of regional anesthesiologists the world over.

ACKNOWLEDGMENTS

The authors thank Mr Liang Liang, BMSc, Research Fellow, Department of Anesthesia, Toronto Western Hospital, Toronto, for his assistance in formatting and editing of images during the preparation of this article.

REFERENCES

1. Sanders RJ, Hammond SL, Rao NM. Thoracic outlet syndrome: a review. *Neurologist*. 2008;14:365–373.
2. Longley DG, Yedlicka JW, Molina EJ, Schwabacher S, Hunter DW, Letourneau JG. Thoracic outlet syndrome: evaluation of the subclavian vessels by color duplex sonography. *AJR Am J Roentgenol*. 1992;158:623–630.
3. Soeding P, Eizenberg N. Review article: anatomical considerations for ultrasound guidance for regional anesthesia of the neck and upper limb. *Can J Anesth*. 2009;56:518–533.
4. Chan VW, Perlas A, Rawson R, Odukoya O. Ultrasound guided supraclavicular brachial plexus block. *Anesth Analg*. 2003;97:1514–1517.
5. Macfarlane AJ, Perlas A, Chan V, Brull R. Eight ball, corner pocket ultrasound guided supraclavicular block: avoiding a scratch. *Reg Anesth Pain Med*. 2008;33:502–503.
6. McCaffrey TV. Evaluation of the thyroid nodule. *Cancer Control*. 2000;7:223–228.
7. Hoang JK, Lee WK, Lee M, Johnson D, Farrell S. US Features of thyroid malignancy: pearls and pitfalls. *Radiographics*. 2007;27:847–860.
8. Thickman DI, Ziskin MC, Goldenberg NJ, Linder BE. Clinical manifestations of the comet tail artifact. *J Ultrasound Med*. 1983;2:225–230.
9. Neal JM, Hebl J, Gerancher JC, et al. Upper extremity regional anesthesia: essentials for our current understanding, 2008. *Reg Anesth Pain Med*. 2009;34:134–170.
10. Lonnquist PA, Mackenzie J, Soni AK, Conacher ID. Paravertebral blockade: failure rate and complications. *Anaesthesia*. 2007;50:813–815.
11. Shanti C, Carlin A, Tyburski J. Incidence of pneumothorax from intercostals nerve block for analgesia in rib fractures. *J Trauma*. 2001;51:536–539.
12. Bouhemad B, Zhang M, Lu Q, Rouby JJ. Clinical review: bedside lung ultrasound in critical care practice. *Crit Care*. 2007;11:205.
13. Lichtenstein DA, Meziere G, Lascols N, et al. Ultrasound diagnosis of occult pneumothorax. *Crit Care Med*. 2005;33:1231–1238.
14. Rutkow IM. Demographic and socioeconomic aspects of hernia repair in the United States in 2003. *Surg Clin North Am*. 2003;83:1045–1051.
15. Jamadar DA, Jacobson JA, Morag Y, et al. Sonography of inguinal region hernias. *AJR Am J Roentgenol*. 2006;187:185–190.
16. Hebbard P, Fujiwara Y, Shibata Y, Royse C. Ultrasound guided transversus abdominis plane (TAP) block. *Anaesth Intensive Care*. 2007;35:616–617.

17. Lloyd T, Tank YM, Benson MD, King S. Diaphragmatic paralysis: the use of M mode ultrasound for diagnosis in adults. *Spinal Cord*. 2006;44:505–508.
18. Baatenburg de Jong RJ, Rongen RJ, Lameris JS, Harthoorn M, Verwoerd CD, Knegt P. Metastatic neck disease. Palpation vs ultrasound examination. *Arch Otolaryngol Head Neck Surg*. 1989; 115:689–690.
19. Vassallo P, Wernecke K, Roos N, Peters PE. Differentiation of benign from malignant superficial lymphadenopathy: the role of high-resolution US. *Radiology*. 1992;183:215–220.
20. Ahuja AT, Ying M. Sonographic evaluation of cervical lymph nodes. *AJR Am J Roentgenol*. 2005;184:1691–1699.
21. Capdevila X, Bringuier S, Borgeat A. Infectious risk of continuous peripheral nerve blocks. *Anesthesiology*. 2009;110:182–188.
22. Hebl JR. The importance and implications of aseptic techniques during regional anesthesia. *Reg Anesth Pain Med*. 2006;31:311–323.
23. Robben SG. Ultrasonography of musculoskeletal infections in children. *Eur Radiol*. 2004;14(suppl 4):L65–L77.
24. Soudack M, Nachtigal A, Gaitini D. Clinically unsuspected foreign bodies: the importance of sonography. *J Ultrasound Med*. 2003;22: 1381–1385.
25. Furness G, Reilly MP, Kuchi S. An evaluation of ultrasound imaging for identification of lumbar intervertebral level. *Anaesthesia*. 2002;57: 277–280.
26. Kil HK, Cho JE, Kim WO, Koo BN, Han SW, Kim JY. Prepuncture ultrasound-measured distance: an accurate reflection of epidural depth in infants and small children. *Reg Anesth Pain Med*. 2007;32:102–106.
27. Carvalho JC. Ultrasound-facilitated epidurals and spinals in obstetrics. *Anesthesiol Clin*. 2008;26:145–158.
28. Yamauchi M, Honma E, Mimura M, Yamamoto H, Takahashi E, Namiki A. Identification of the lumbar intervertebral level using ultrasound imaging in a post-laminectomy patient. *J Anesth*. 2006;20:231–233.

